*Article*

# Application of Neural Network and Dual-Energy Radiation-Based Detection Techniques to Measure Scale Layer Thickness in Oil Pipelines Containing a Stratified Regime of Three-Phase Flow

Abdulilah Mohammad Mayet [1], Tzu-Chia Chen [2,3,*], Ijaz Ahmad [4,*], Elsayed Tag Eldin [5],
Ali Awadh Al-Qahtani [1], Igor M. Narozhnyy [6], John William Grimaldo Guerrero [7] and Hala H. Alhashim [8]

[1]  Electrical Engineering Department, King Khalid University, Abha 61411, Saudi Arabia
[2]  College of Management and Design, Ming Chi University of Technology, New Taipei City 243303, Taiwan
[3]  International College, Krirk University, Bangkok, 3 Ram Inthra Rd, Khwaeng Anusawari, Khet Bang Khen, Krung Thep Maha Nakhon 10220, Thailand
[4]  Shenzhen College of Advanced Technology, University of Chinese Academy of Sciences (UCAS), Shenzhen 518055, China
[5]  Electrical Engineering Department, Faculty of Engineering & Technology, Future University in Egypt, New Cairo 11845, Egypt
[6]  Department of Commercialization of Intellectual Activity Resultse Center for Technology Transfer of RUDN University, Mining Oil and Gas Department, RUDN University, 117198 Moscow, Russia
[7]  Department of Energy, Universidad de la Costa, Barranquilla 080001, Colombia
[8]  Department of Physics, College of Science, Imam Abdulrahman Bin Faisal University, Dammam 31441, Saudi Arabia
*   Correspondence: tzuchiachen1688@gmail.com (T.-C.C.); ijaz@siat.ac.cn (I.A.)

**Abstract:** Over time, oil pipes are scaled, which causes problems such as a reduction in the effective diameter of the oil pipe, an efficiency reduction, waste of energy, etc. Determining the exact value of the scale inside the pipe is very important in order to take timely action and to prevent the mentioned problems. One accurate detection methodology is the use of non-invasive systems based on gamma-ray attenuation. For this purpose, in this research, a scale thickness detection system consisting of a test pipe, a dual-energy gamma source ($^{241}$Am and $^{133}$Ba radioisotopes), and two sodium iodide detectors were simulated using the Monte Carlo N Particle (MCNP) code. In the test pipe, three-phase flow consisting of water, gas, and oil was simulated in a stratified flow regime in volume percentages in the range from 10% to 80%. In addition, a scale with different thicknesses from 0 to 3 cm was placed inside the pipe, and gamma rays were irradiated onto the pipe; on the other side of the pipe, the photon intensity was recorded by the detectors. A total of 252 simulations were performed. From the signal received by the detectors, four characteristics were extracted, named the Photopeaks of $^{241}$Am and $^{133}$Ba for the first and second detectors. After training many different Multi-Layer Perceptron(MLP) neural networks with various architectures, it was found that a structure with two hidden layers could predict the connection between the input, extracted features, and the output, scale thickness, with a Root Mean Square Error (RMSE) of less than 0.06. This low error value guarantees the effectiveness of the proposed method and the usefulness of this method for the oil and petrochemical industry.

**Keywords:** three-phase flow; scale layer thickness; volume fraction independent; MLP neural network

**MSC:** 68T07; 92B20

## 1. Introduction

Scale deposition inside oil pipes has caused loads of issues in many oil fields in the world. Scale formation reduces the effective cross section of pipelines and makes the flow

of oil products difficult. This factor causes pumps and various equipment to not work properly. Increasing the amount of scale inside the pipe and not identifying it in time can even cause an emergency shutdown, damage the oil equipment, increase repair costs, and decrease efficiency. Therefore, it is necessary to design accurate detection systems to determine the amount of scale inside the pipe. Researchers always refer to gamma-ray attenuation systems as the golden standard in determining the various parameters of multi-phase flows [1–8]. In [1], a laboratory structure compromised of a cesium source, and a test pipe was applied. The researchers applied the two-phase flow in three regimes: stratified, annular, and bubbly. By using the counts in both transmitted detectors as input to the Radial Basis Function (RBF), they succeeded to estimate volume percentages and to classify the flow regimes. In [2], Roshni et al. used three Group Method of Data Handling (GMDH) networks to increase the accuracy in determining the volume percentages and in recognizing the type of flow regimes in three-phase fluids. Although the accuracy increased, a large computational load was imposed on the system. In 2016, Roshni et al. [3] used a $^{60}$Co source and a detector to determine the type of flow regimes and volume percentages. Failure to extract appropriate characteristics from the recorded signals caused low accuracy in determining the mentioned parameters. In 2019 [4], researchers used the Jaya optimization algorithm to predict the volume percentages. Following the introduction of a system to accurately determine volume percentages and classification of flow regimes, Sattari et al. [5] used a cesium source, a test pipe, and two NaI detectors. By extracting time characteristics and by chossing the most effective characteristic, they reduced the computational load on the neural network and introduced an accurate system. In their subsequent research [6], they investigated the use of a GMDH neural network to detect the type of flow regimes and to predict volume percentages. High accuracy was achieved when determining the volume percentages, but failure to consider the amount of scale inside the pipe is one of the gaps in the mentioned research. Alamoudi and colleagues [7] tried to detect the amount of scale thickness in the oil pipe by using a dual-energy source including Ba-133 and Cs-137. They simulated a two-phase flow in different regimes. They considered Gamma peak counts of Cs-137 and Ba-133 from the first detector and total counts from the second detector as inputs of the RBF neural network and succeeded to estimate the thickness of the scale with a Root Mean Square Error (RMSE) of 0.22. In [8], the authors modelled a three-phase flow regime in the annular regime. Considering the scale thickness deposited inside the pipe, they investigated different volume percentages. Finally, by extracting the Photopeaks of $^{241}$Am and $^{133}$Ba recorded in the two detectors and considering them as the inputs of an RBF neural network, they predicted the amount of scale inside the pipe with an RMSE of less than 0.09. In recent years, due to problems with using radioisotopes including the need to use protective clothing when dealing with this device (due to the inability to turn it off), problems in transportation, etc., researchers used X-ray tubes to determine the parameters of multiphase flows [9–12]. In [9], the researchers determined the regime type and volume percentage of two-phase flows using an X-ray tube and a sodium iodide detector. They extracted temporal characteristics from the signals received by the detector and used these characteristics to train two Multi-Layer Perceptron (MLP) neural networks. In [10], three-phase flows were investigated. In this way, three annular, stratified, and homogeneous flow regimes were simulated in different volume percentages. In this research, three RBF neural networks were trained with the frequency characteristics of the received signals, which were relatively accurate. In [11], an X-ray tube was used to design a control system. Four petroleum products, which are blended two by two at various volume rates, were modelled by the MCNP code. The recorded signals were placed as inputs of three MLP neural networks to predict the volume ratio of three products. The researchers stated that the volume ratio of the fourth product could be calculated by having the volume ratio as the other three products. Although the method introduced predicted the type and number of products, the lack of feature extraction techniques used prevented high accuracy. Developing upon previous research [11], Balubaid et al. [12] used wavelet transforms for feature extraction. This research not only increased

the system's accuracy but also reduced the computational load. Further studies in the field of multiphase flowmeters can be found in [13–19]. In [20], research has been conducted to determine the scale value inside the pipe. Although the number of detectors was reduced to one, the system error was relatively high. Recently, neural networks have been used in determining different parameters in different fields of science, such as Unsupervised learning-based subset simulation with customizable intermediate failure probability for reliability analysis [21], estimating combined cycle power plants' electrical output [22]; concrete made with synthetic sand's compressive strength prediction [23]; optimization of existing metaheuristics for concrete slump modeling [24]; using an equilibrium optimization model to estimate the tensile strength at a fracture of concrete [25]; identifying structural damage with an innovative artificial bee colony algorithm [26]; and laser-cut geometries for soft electroactuators [27].

In the current research, inspired by previous studies, an attempt was made to design a high-precision system to detect the scale value inside the pipe. For this purpose, a three-phase flow regime consisting of water, gas, and oil in different volume percentages was simulated. Different values of scale thickness were considered in each simulation. A dual-energy source ($^{241}$Am and $^{133}$Ba) and two detectors were positioned on both sides of the test pipe. From the signals received from each detector, two characteristics of the Photopeaks of $^{241}$Am and $^{133}$Ba were extracted. These features were applied to the inputs of the MLP neural network while the desired output was the scale thickness value inside the pipe. The main contributions of the present investigation can be categorized as following:

1. Increasing accuracy in the detection system;
2. Obtaining the value of scale thickness in the event that a three-phase flow passes through the oil pipe;
3. Investigating the performance of the characteristics of the Photopeaks of $^{241}$Am and $^{133}$Ba for the first and second detectors when determining the thickness of the scale;
4. Reducing the computational load by extracting effective features.

## 2. Simulated Detection System

The configuration of the detection system proposed in this investigation is simulated by the MCNP code [28]. In recent years, the use of this platform for simulating radiation-based systems has been greatly appreciated by researchers [29–32]. The detection system consists of a dual-energy source, a steel test pipe, and two sodium iodide detectors. The gamma sources include $^{241}$Am and $^{133}$Ba radioisotopes. The test pipe used for simulating the three-phase flow in the stratified regime as well as the deposited scale has an inner diameter of 10 cm and a thickness of 0.5 cm. Two 2.54 cm $\times$ 2.54 cm detectors were located at a distance of 30 cm from the source in such a way that one of them was exactly in front of the source and the other was at an angle of 7° to the hypothetical line between the source and the first detector. As mentioned, three-phase flow was simulated in a stratified regime consisting of water, oil, and gas in volume percentages between 10% and 80%. Barium sulfate (BaSO4), which has a density of 4.5 g·cm$^{-3}$, was used to simulate the scale at thicknesses of 0, 0.05, 1, 1.5, 2, 2.5, and 3 cm inside a cylindrical pipe. The water, oil, and gas considered in this simulation had densities of 1, 0.826, and 0.00125 g·cm$^{-3}$. The structure simulated in this study was validated with the experimental structure implemented in [1]. A two-phase flow was performed in the annular regime, and the same structure was implemented in the MCNP code. The registered counts obtained from the detectors of the simulation structure and the experimental structure were compared with each other. It was observed that there is an acceptable match between the two. Seven scale thicknesses $\times$ 36 different volume percentages = 252 simulations were performed. From each simulation, four characteristics, named the Photopeaks of $^{241}$Am and $^{133}$Ba for the first and second detectors, were extracted; in total, a matrix of 4 $\times$ 252 was obtained for neural network training. The desired output of this research was the thickness of the scale inside the pipe. The simulated configuration is depicted in Figure 1. Figures 2 and 3 show ternary surface plots related to the count under the Photopeaks of $^{241}$Am and $^{133}$Ba in the second detector

for various combined gas, oil, and water volume fractions at the thickness scales of 0 and 1.5 cm, respectively. As can be observed from the comparison of these two figures, with an increase in the thickness of the scale, the count recorded by the detectors decreases, which can be an important factor in distinguishing the selected characteristics. The graph of extracted characteristics in terms of scale thickness in constant volume percentage (10% gas, 40% oil, and 50% water) is shown in Figure 4.
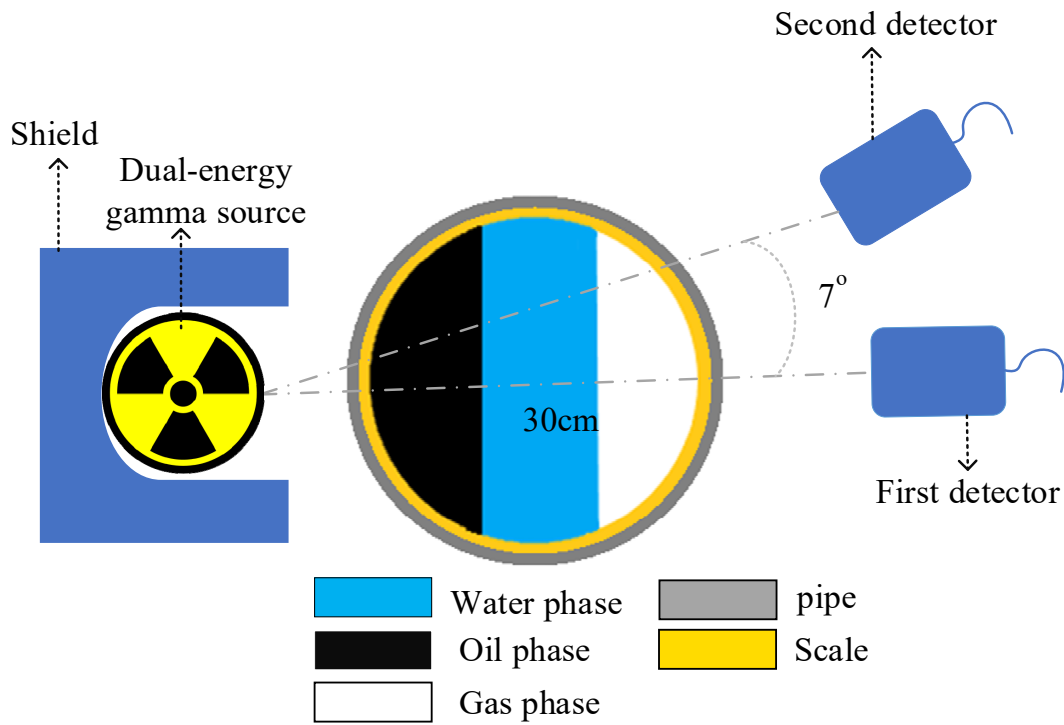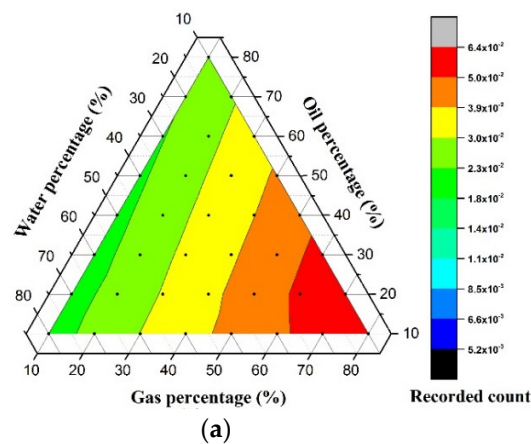


**Figure 1.** The configuration of the modelled system.



(**a**)

**Figure 2.** *Cont.*

**Figure 2.** Recorded counts under Photopeaks of (**a**) $^{241}$Am and (**b**) $^{133}$Ba radioisotope in the second detector for different combed oil, gas and water volume fractions at thickness scale of 0 cm.
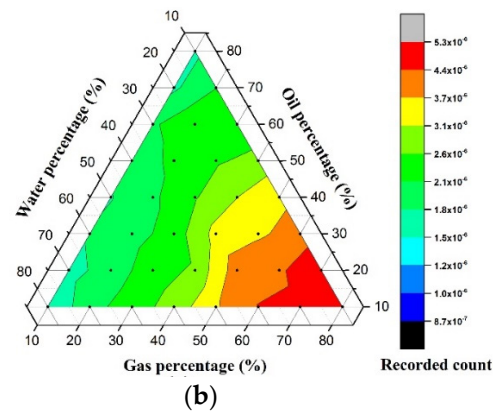


**Figure 3.** Recorded counts under Photopeaks of (**a**) $^{241}$Am and (**b**) $^{133}$Ba radioisotope in the second detector for different combined oil, gas and water volume fractions at thickness scale of 1.5 cm.
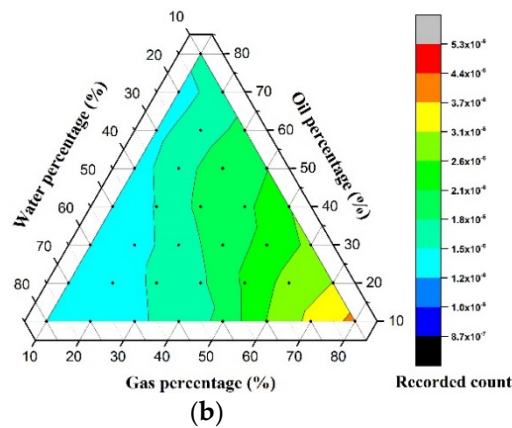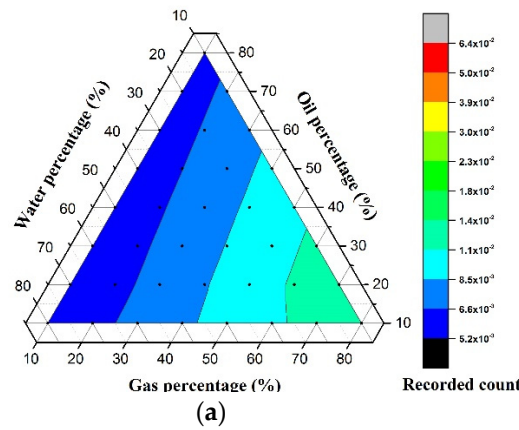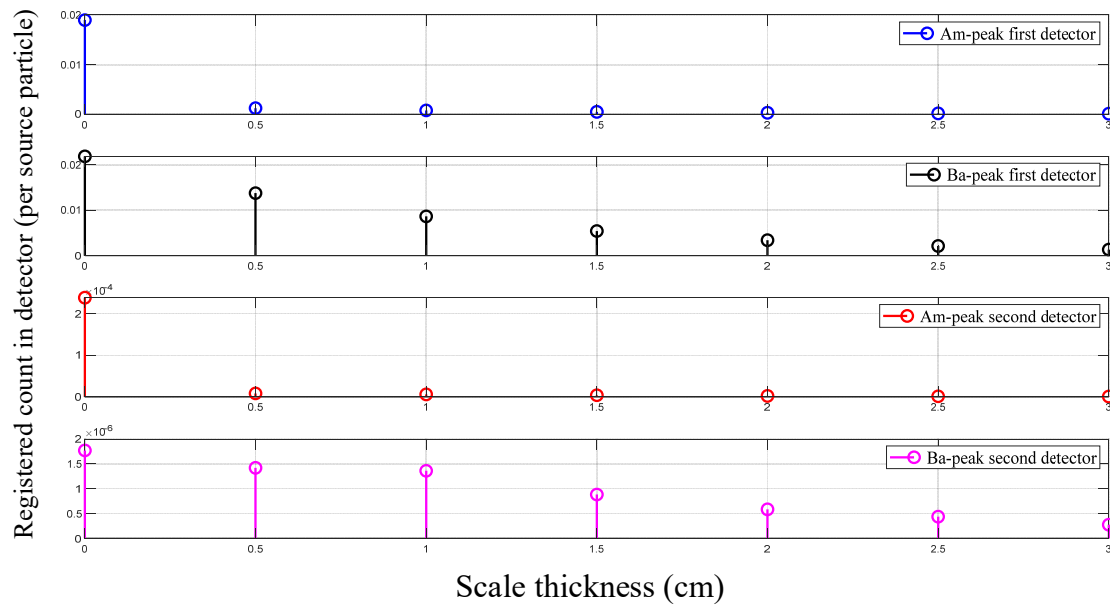
**Figure 4.** Extracted characteristics in terms of scale thickness in constant volume percentage (10% gas, 40% oil, and 50% water).

## 3. MLP Neural Network

Millions of neurons, or little computer units, make up the human brain. These neurons are all linked to one another. Dendrites, which are branching on neurons, are where other neurons send information. The nucleus, which is a neuron's processing center, converts input data into output data that are then sent to other neurons via an output line called an axon. These all take place in the biological and physiological realms. One of the most popular approaches developed by researchers to model this function in mathematics is the MLP neural network. There are input and output layers in this network's structure. Between these two layers, there may be a variety of hidden layers. A number of mathematical operations are carried out in the hidden layers and are introduced as the activation function. The type and level of nonlinearity of the available data determine the structure and number of these layers, and the type of activation function. Numerous studies have used intelligent computing systems to determine various parameters in different fields of science [33–53]. The output of neurons in the mathematical formulation of neurons is as follows [54,55]:

$$n_l = \sum_{i=1}^{u} x_i w_{ij} + b \ j = 1, 2, \cdots, m \tag{1}$$

$$u_j = f\left(\sum_{i=1}^{u} x_i w_{ij} + b\right) j = 1, 2, \cdots, m \tag{2}$$

$$output = \sum_{n=1}^{j} (u_n w_n) + b \tag{3}$$

in which $x$ presents the input parameters; the weighting factor, the bias term, and the activation function are indicated as $w$, $b$, and $f$, respectively. In the design of artificial neural networks, in order to avoid the problem of over-training and under-training, the available data are divided into three categories: training, testing and validation. The training data include the majority of the data, and these data are used in order for the neural network to see them and fit them. Validation data are used to ensure the correct training process in such a way that these data are used for network testing. The test data are applied to the neural network at the end of the neural network training process in order to ensure the accuracy of performance. When a neural network can work properly in operational

conditions, it performs well against all three introduced categories. The number of training, validation, and test data in this research are 176, 38, and 38, respectively.

## 4. Results and Discussion

The four features introduced in the former section were applied to the input of the MLP network, which consisted of a $4 \times 252$ matrix. The output of the neural network was the thickness of the scale inside the pipe, which is a $1 \times 252$ matrix. Several neural networks with different numbers of hidden layers and different numbers of neurons in the hidden layers were implemented, and a structure including two hidden layers, 10 neurons in the first hidden layer and 5 neurons in the second hidden layer, could accurately estimate the thickness of the scale inside the pipe. The structure of the designed MLP network is shown in Figure 5. To calculate the error value of the implemented network, two criteria, Mean Square Error (MSE) and RMSE, were considered. The equations of these criteria are as follows:

$$MSE = \frac{\sum_{j=1}^{N}\big(X_j(Exp) - X_j(Pred)\big)^2}{N} \tag{4}$$

$$RMSE = \left[\frac{\sum_{j=1}^{N}\big(X_j(Exp) - X_j(Pred)\big)^2}{N}\right]^{0.5} \tag{5}$$

in which *N* indicates data number; '*X (Exp)*' and '*X (Pred)*' illustrate the experimental and predicted (using network) values, respectively.
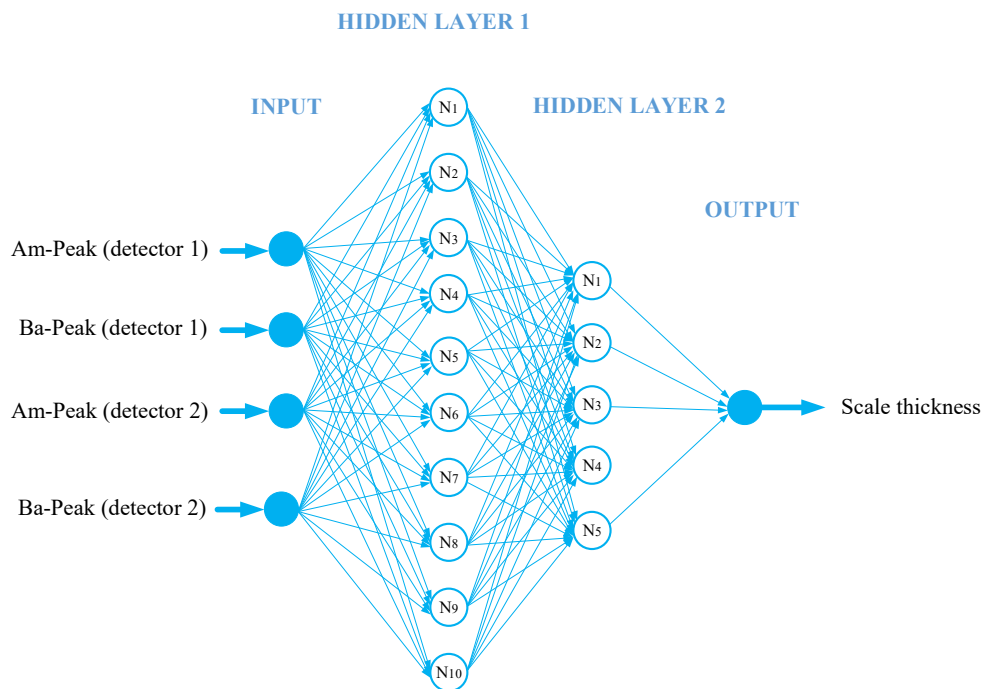


**Figure 5.** Structure of designed MLP neural network.

In order to show the correct performance of the neural network, three fitting, regression, and error histogram graphs were plotted for three categories: training, validation and testing data (Figure 6). In the fitting diagram, the desired output is shown with a red dashed line and the network output is shown with a black line. In the second diagram, the desired output is visible as a red dashed line, and the outputs of the neural network is visible as black squares. This diagram is presented as a regression diagram. The horizontal axis in this diagram shows the data number, and the vertical axis shows the thickness of the scale. The histogram diagram shows the value of error distribution; the distribution of this

value is around the zero number, indicating the low error value of the designed network. Table 1 shows the characteristics and errors of the designed neural network. Table 2 shows a comparison in terms of the amount of error in the designed detection system with the systems introduced in previous research. The general process of the presented methodology to determine the thickness of the scale inside the pipe can be seen in Figure 7. According to this figure, in the first stage of the configuration of the system, the flows passing through the pipe and the different thicknesses of the scale inside the pipe were simulated by the MCNP code, and the signals received by the detectors were labeled. Then, the received signals were processed and four characteristics of the Photopeaks of $^{241}$Am and $^{133}$Ba for the first and second detectors were extracted from the signals of each simulation. The characteristics obtained were assigned as inputs of the MLP neural network to estimate the scale thickness within the pipe. After training the neural network, in order to ensure correct functioning of this network, the output results of the network were compared with the desired output.
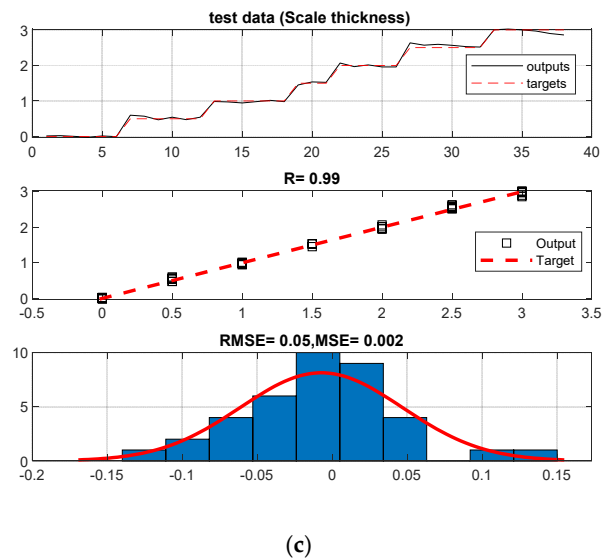


(**a**)



(**b**)

**Figure 6.** *Cont.*

(**c**)
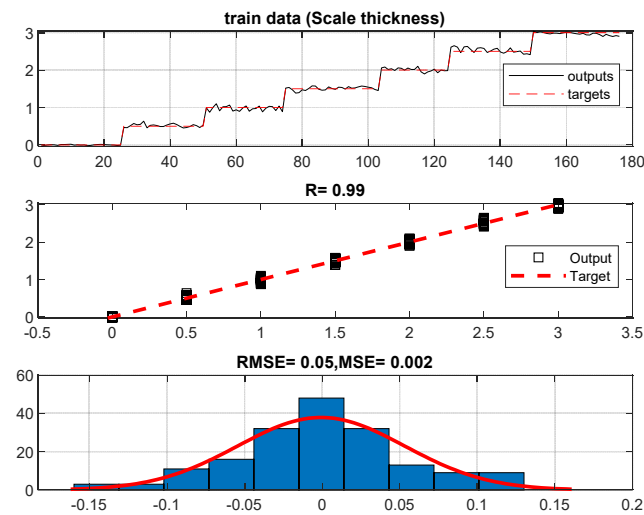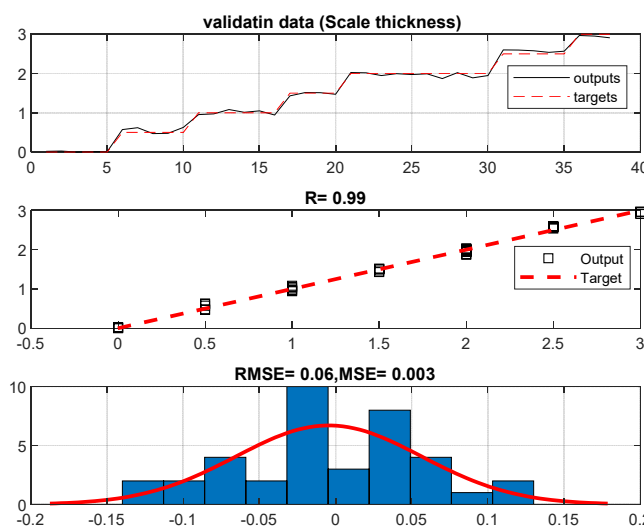
**Figure 6.** Fitting, regression, and error histogram diagram for (**a**) training, (**b**) validation, and (**c**) testing data.

**Table 1.** Designed network charectristics.

| Type of Artificial Neural Network (ANN) | MLP | | |
|---|---|---|---|
| Input layer neurons | 4 | | |
| The first hidden layer neurons | 10 | | |
| The second hidden layer neurons | 5 | | |
| Output layer neurons | 1 | | |
| The number of epochs | 600 | | |
| Hidden neuron activation function | Tansig | | |
| MSE of predicting scale thickness | **Training data** | **Validation data** | **Test data** |
| | 0.002 | 0.003 | 0.002 |
| RMSE of predicting scale thickness | 0.05 | 0.06 | 0.05 |

**Table 2.** A comparison of the accuracy of previous studies and the proposed detection system.

| Ref | Extracted Features | Type of Neural Network | Maximum MSE | Maximum RMSE |
|---|---|---|---|---|
| [6] | Time features | GMDH | 1.24 | 1.11 |
| [5] | Time features | MLP | 0.21 | 0.46 |
| [56] | No feature extraction | GMDH | 7.34 | 2.71 |
| [57] | Frequency features | MLP | 0.67 | 0.82 |
| [58] | No feature extraction | MLP | 17.05 | 4.13 |
| [59] | No feature extraction | MLP | 2.56 | 1.6 |
| [60] | Compton continuum and counts under full energy peaks of 1173 and 1333 keV | RBF | 37.45 | 6.12 |
| [61] | Full energy peak, photon counts of Compton edge in transmission detector and total count in the scattering detector | MLP | 1.08 | 1.04 |
| **Current study** | Photopeaks of $^{241}$Am and $^{133}$Ba for the first and second detectors | MLP | 0.003 | 0.06 |
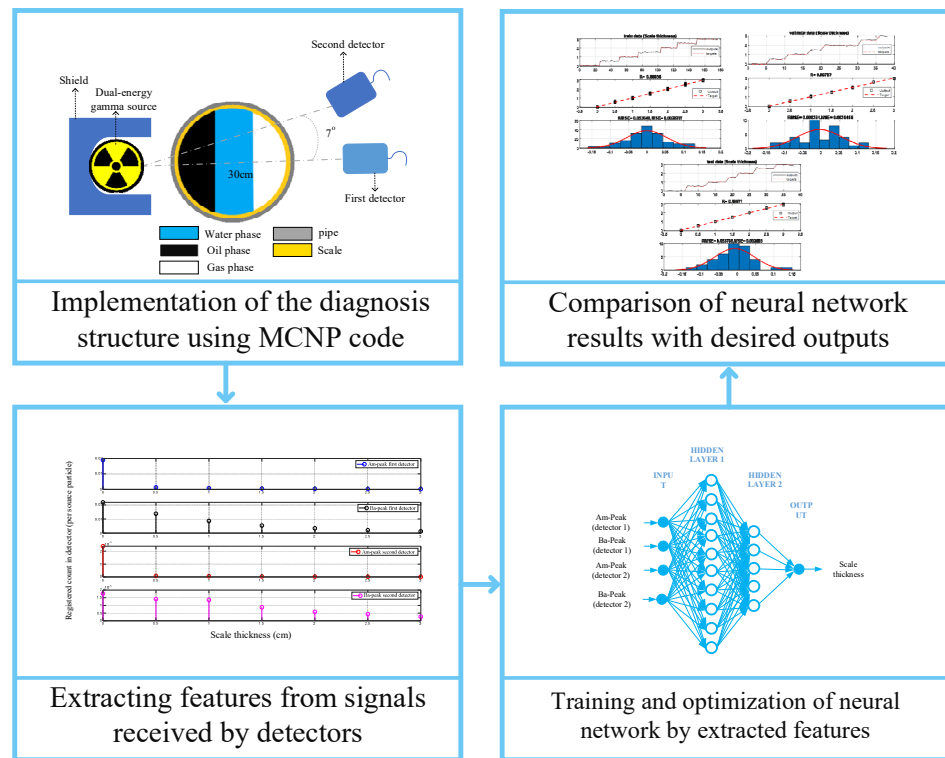
**Figure 7.** The general trend of the presented methodology to determine the scale thickness inside the pipe.

The low error value obtained in this research was due to the correct processing of the signals obtained and the training of the neural network with effective characteristics of the signal. A very basic limitation in this research is the use of radioisotope devices, which requires protective equipment and clothing due to the harmful effects on the human body. Investigating different characteristics such as time, frequency, and wavelet transform characteristics and examining the performance of different neural networks for productivity in future research are strongly recommended to researchers in this field.

## 5. Conclusions

It is important to detect the amount of scale deposited inside oil pipes because failure to address this important issue can cause problems for the operation of all oil equipment and can even cause an emergency shutdown of the entire oil field. Therefore, designing an accurate system to detect the amount of scale inside the pipes and taking timely action to solve this problem could play a vital role in improving the performance of the oil industry. In this research, in order to introduce an accurate system, the gamma-ray attenuation technique was used to measure the thickness of the scale inside the pipe. The structure of the detection system comprised of a dual-energy source and two sodium iodide detectors, which are placed on both sides of the pipe in which the amount of the deposited scale is to be measured. This structure was simulated using the MCNP code. Three-phase flow in a stratified regime was simulated throughout a range of volume fractions from 10% to 80%, with corresponding scale values explored from 0 cm to 3 cm. From the signals received from all the simulations, four features named the Photopeaks of $^{241}$Am and $^{133}$Ba for both detectors were extracted and used in the design of a neural network. An MLP neural network was trained in a condition where the mentioned features were considered as input and the scale thickness value was considered as output. This neural network was capable to estimate the thickness of the scale with an RMSE of 0.06, that is a quite low error in comparison with the former studies. The use of radioisotope devices in this research is the biggest challenge because it is necessary to use protective clothing to

maintain the health of those working with these devices. Investigating time, frequency, wavelet transform, etc., and investigating the performance of different neural networks including deep neural networks can be introduced as the subject of future research. The detection system introduced in this research is very useful for detecting the amount of scale inside a pipe and solving the mentioned problems caused by the scale depositing, and its use for oil industries is strongly recommended.

**Author Contributions:** Conceptualization, I.A.; Formal analysis, E.T.E. and H.H.A.; Funding acquisition, E.T.E.; Investigation, T.-C.C.; Methodology, A.M.M., T.-C.C., A.A.A.-Q. and H.H.A.; Resources, J.W.G.G.; Software, A.M.M., A.A.A.-Q. and H.H.A.; Writing—original draft, I.A., I.M.N. and J.W.G.G. All authors have read and agreed to the published version of the manuscript.

**Data Availability Statement:** This study did not report any data.

**Conflicts of Interest:** The authors declare no conflict of interest.

## References

1. Nazemi, E.; Roshani, G.H.; Feghhi, S.A.H.; Setayeshi, S.; Zadeh, E.E.; Fatehi, A. Optimization of a method for identifying the flow regime and measuring void fraction in a broad beam gamma-ray attenuation technique. *Int. J. Hydrogen Energy* **2016**, *41*, 7438–7444. [CrossRef]
2. Roshani, M.; Phan, G.; Roshani, G.H.; Hanus, R.; Nazemi, B.; Corniani, E.; Nazemi, E. Combination of X-ray tube and GMDH neural network as a nondestructive and potential technique for measuring characteristics of gas-oil–water three phase flows. *Measurement* **2021**, *168*, 108427. [CrossRef]
3. Roshani, G.H.; Nazemi, E.; Feghhi, S.A.H. Investigation of using 60Co source and one detector for determining the flow regime and void fraction in gas–liquid two-phase flows. *Flow Meas. Instrum.* **2016**, *50*, 73–79. [CrossRef]
4. Roshani, G.H.; Karami, A.; Nazemi, E. An intelligent integrated approach of Jaya optimization algorithm and neuro-fuzzy network to model the stratified three-phase flow of gas–oil–water. *Comput. Appl. Math.* **2019**, *38*, 5. [CrossRef]
5. Sattari, M.A.; Roshani, G.H.; Hanus, R.; Nazemi, E. Applicability of time-domain feature extraction methods and artificial intelligence in two-phase flow meters based on gamma-ray absorption technique. *Measurement* **2021**, *168*, 108474. [CrossRef]
6. Sattari, M.A.; Roshani, G.H.; Hanus, R. Improving the structure of two-phase flow meter using feature extraction and GMDH neural network. *Radiat. Phys. Chem.* **2020**, *171*, 108725. [CrossRef]
7. Alamoudi, M.; Sattari, M.A.; Balubaid, M.; Eftekhari-Zadeh, E.; Nazemi, E.; Taylan, O.; Kalmoun, E.M. Application of Gamma Attenuation Technique and Artificial Intelligence to Detect Scale Thickness in Pipelines in Which Two-Phase Flows with Different Flow Regimes and Void Fractions Exist. *Symmetry* **2021**, *13*, 1198. [CrossRef]
8. Taylan, O.; Abusurrah, M.; Amiri, S.; Nazemi, E.; Eftekhari-Zadeh, E.; Roshani, G.H. Proposing an Intelligent Dual-Energy Radiation-Based System for Metering Scale Layer Thickness in Oil Pipelines Containing an Annular Regime of Three-Phase Flow. *Mathematics* **2021**, *9*, 2391. [CrossRef]
9. Basahel, A.; Sattari, M.A.; Taylan, O.; Nazemi, E. Application of Feature Extraction and Artificial Intelligence Techniques for Increasing the Accuracy of X-ray Radiation Based Two Phase Flow Meter. *Mathematics* **2021**, *9*, 1227. [CrossRef]
10. Taylan, O.; Sattari, M.A.; Elhachfi Essoussi, I.; Nazemi, E. Frequency Domain Feature Extraction Investigation to Increase the Accuracy of an Intelligent Nondestructive System for Volume Fraction and Regime Determination of Gas-Water-Oil Three-Phase Flows. *Mathematics* **2021**, *9*, 2091. [CrossRef]
11. Roshani, G.H.; Ali, P.J.M.; Mohammed, S.; Hanus, R.; Abdulkareem, L.; Alanezi, A.A.; Sattari, M.A.; Amiri, S.; Nazemi, E.; Eftekhari-Zadeh, E.; et al. Simulation Study of Utilizing X-ray Tube in Monitoring Systems of Liquid Petroleum Products. *Processes* **2021**, *9*, 828. [CrossRef]
12. Balubaid, M.; Sattari, M.A.; Taylan, O.; Bakhsh, A.A.; Nazemi, E. Applications of Discrete Wavelet Transform for Feature Extraction to Increase the Accuracy of Monitoring Systems of Liquid Petroleum Products. *Mathematics* **2021**, *9*, 3215. [CrossRef]
13. Hanus, R.; Zych, M.; Kusy, M.; Jaszczur, M.; Petryka, L. Identification of liquid-gas flow regime in a pipeline using gamma-ray absorption technique and computational intelligence methods. *Flow Meas. Instrum.* **2018**, *60*, 17–23. [CrossRef]
14. El Abd, A. Intercomparison of gamma ray scattering and transmission techniques for gas volume fraction measurements in two phase pipe flow. *Nucl. Instrum. Methods Phys. Res. A* **2014**, *735*, 260–266. [CrossRef]
15. Salgado, C.M.; Brandão, L.E.B.; Conti, C.C.; Salgado, W.L. Density prediction for petroleum and derivatives by gamma-ray attenuation and artificial neural networks. *Appl. Radiat. Isot.* **2016**, *116*, 143–149. [CrossRef]
16. Mosorov, V.; Zych, M.; Hanus, R.; Petryka, L. Modelling of dynamic experiments in MCNP5 environment. *Appl. Radiat. Isot.* **2016**, *112*, 136–140. [CrossRef]

17. Salgado, C.M.; Brandao, L.E.B.; Pereira, C.M.N.A.; Salgado, W.L. Salinity independent volume fraction prediction in annular and stratified (water-gas-oil) multiphase flows using artificial neural networks. *Prog. Nucl. Energy* **2014**, *76*, 17–23. [CrossRef]

18. Mosorov, V.; Zych, M.; Hanus, R.; Sankowski, D.; Saoud, A. Improvement of Flow Velocity Measurement Algorithms Based on Correlation Function and Twin Plane Electrical Capacitance Tomography. *Sensors* **2020**, *20*, 306. [CrossRef]

19. Salgado, C.M.; Pereira, C.M.N.A.; Schirru, R.; Brandao, L.E.B. Flow regime identification and volume fraction prediction in multiphase flows by means of gamma-ray attenuation and artificial neural networks. *Prog. Nucl. Energy* **2010**, *52*, 555–562. [CrossRef]

20. Mayet, A.M.; Chen, T.-C.; Alizadeh, S.M.; Al-Qahtani, A.A.; Alanazi, A.K.; Ghamry, N.A.; Alhashim, H.H.; Eftekhari-Zadeh, E. Optimizing the gamma ray-based detection system to measure the scale thickness in three-phase flow through oil and petrochemical pipelines in view of stratified regime. *Processes* **2022**, *10*, 1866. [CrossRef]

21. Zhao, Y.; Zeyu, W. Subset simulation with adaptable intermediate failure probability for robust reliability analysis: An unsupervised learning-based approach. *Struct. Multidiscip. Optim.* **2022**, *65*, 172. [CrossRef]

22. Zhao, Y.; Loke, K.F. Predicting Electrical Power Output of Combined Cycle Power Plants Using a Novel Artificial Neural Network Optimized by Electrostatic Discharge Algorithm. *Measurement* **2022**, *198*, 111405. [CrossRef]

23. Zhao, Y.; Hesong, H.; Chaolin, S.; Zeyu, W. Predicting compressive strength of manufactured-sand concrete using conventional and metaheuristic-tuned artificial neural network. *Measurement* **2022**, *194*, 110993. [CrossRef]

24. Foong, L.K.; Yinghao, Z.; Chengzong, B.; Chengyong, X. Efficient metaheuristic-retrofitted techniques for concrete slump simulation. *Smart Struct. Syst. Int. J.* **2021**, *27*, 745–759.

25. Zhao, Y.; Zhong, X.; Foong, L.K. Predicting the splitting tensile strength of concrete using an equilibrium optimization model. *Steel Compos. Struct. Int. J.* **2021**, *39*, 81–93.

26. Zhao, Y.; Yan, Q.; Yang, Z.; Yu, X.; Jia, B. A novel artificial bee colony algorithm for structural damage detection. *Advances Civil Eng.* **2020**, *2020*, 3743089. [CrossRef]

27. Yan, B.; Ma, C.; Zhao, Y.; Hu, N.; Guo, L. Geometrically Enabled Soft Electroactuators via Laser Cutting. *Adv. Eng. Mater.* **2019**, *21*, 1900664. [CrossRef]

28. Pelowitz, D.B. *MCNP-X TM User's Manual, Version 2.5.0*; LA-CP-05e0369; Los Alamos National Laboratory: Los Alamos, NM, USA, 2005.

29. Hosseini, S.; Taylan, O.; Abusurrah, M.; Akilan, T.; Nazemi, E.; Eftekhari-Zadeh, E.; Bano, F.; Roshani, G.H. Application of Wavelet Feature Extraction and Artificial Neural Networks for Improving the Performance of Gas–Liquid Two-Phase Flow Meters Used in Oil and Petrochemical Industries. *Polymers* **2021**, *13*, 3647. [CrossRef]

30. Sattari, M.A.; Korani, N.; Hanus, R.; Roshani, G.H.; Nazemi, E. Improving the performance of gamma radiation based two phase flow meters using optimal time characteristics of the detector output signal extraction. *J. Nucl. Sci. Technol.* **2020**, *41*, 42–54.

31. Iliyasu, A.M.; Mayet, A.M.; Hanus, R.; El-Latif, A.A.A.; Salama, A.S. Employing GMDH-Type Neural Network and Signal Frequency Feature Extraction Approaches for Detection of Scale Thickness inside Oil Pipelines. *Energies* **2022**, *15*, 4500. [CrossRef]

32. Mayet, A.M.; Salama, A.S.; Alizadeh, S.M.; Nesic, S.; Guerrero, J.W.G.; Eftekhari-Zadeh, E.; Nazemi, E.; Iliyasu, A.M. Applying Data Mining and Artificial Intelligence Techniques for High Precision Measuring of the Two-Phase Flow's Characteristics Independent of the Pipe's Scale Layer. *Electronics* **2022**, *11*, 459. [CrossRef]

33. Lalbakhsh, A.; Mohamadpour, G.; Roshani, S.; Ami, M.; Roshani, S.; Sayem, A.S.; Alibakhshikenari, M.; Koziel, S. Design of a compact planar transmission line for miniaturized rat-race coupler with harmonics suppression. *IEEE Access* **2021**, *9*, 129207–129217. [CrossRef]

34. Hookari, M.; Roshani, S.; Roshani, S. High-efficiency balanced power amplifier using miniaturized harmonics suppressed coupler. *Int. J. RF Microw. Comput.-Aided Eng.* **2020**, *30*, e22252. [CrossRef]

35. Lotfi, S.; Roshani, S.; Roshani, S.; Gilan, M.S. Wilkinson power divider with band-pass filtering response and harmonics suppression using open and short stubs. *Frequenz* **2020**, *74*, 169–176. [CrossRef]

36. Jamshidi, M.; Siahkamari, H.; Roshani, S.; Roshani, S. A compact Gysel power divider design using U-shaped and T-shaped resonators with harmonics suppression. *Electromagnetics* **2019**, *39*, 491–504. [CrossRef]

37. Roshani, S.; Jamshidi, M.B.; Mohebi, F.; Roshani, S. Design and modeling of a compact power divider with squared resonators using artificial intelligence. *Wirel. Pers. Commun.* **2021**, *117*, 2085–2096. [CrossRef]

38. Roshani, S.; Azizian, J.; Roshani, S.; Jamshidi, M.B.; Parandin, F. Design of a miniaturized branch line microstrip coupler with a simple structure using artificial neural network. *Frequenz* **2022**, *76*, 255–263. [CrossRef]

39. Khaleghi, M.; Salimi, J.; Farhangi, V.; Moradi, M.J.; Karakouzian, M. Application of Artificial Neural Network to Predict Load Bearing Capacity and Stiffness of Perforated Masonry Walls. *CivilEng* **2021**, *2*, 48–67. [CrossRef]

40. Dabiri, H.; Farhangi, V.; Moradi, M.J.; Zadehmohamad, M.; Karakouzian, M. Applications of Decision Tree and Random Forest as Tree-Based Machine Learning Techniques for Analyzing the Ultimate Strain of Spliced and Non-Spliced Reinforcement Bars. *Appl. Sci.* **2022**, *12*, 4851. [CrossRef]

41. Zych, M.; Petryka, L.; Kępński, J.; Hanus, R.; Bujak, T.; Puskarczyk, E. Radioisotope investigations of compound two-phase flows in an ope channel. *Flow Meas. Instrum.* **2014**, *35*, 11–15. [CrossRef]

42. Zych, M.; Hanus, R.; Wilk, B.; Petryka, L.; Świsulski, D. Comparison of noise reduction methods in radiometric correlation measurements of two-phase liquid-gas flows. *Measurement* **2018**, *129*, 288–295. [CrossRef]

43. Golijanek-Jędrzejczyk, A.; Mrowiec, A.; Hanus, R.; Zych, M.; Heronimczak, M.; Świsulski, D. Uncertainty of mass flow measurement using centric and eccentric orifice for Reynolds number in the range 10,000 ≤ Re ≤ 20,000. *Measurement* **2020**, *160*, 107851. [CrossRef]

44. Mayet, A.; Hussain, M. Amorphous WNx Metal For Accelerometers and Gyroscope. In Proceedings of the MRS Fall Meeting, Boston, MA, USA, 30 November–5 December 2014.

45. Mayet, A.; Hussain, A.; Hussain, M. Three-terminal nanoelectromechanical switch based on tungsten nitride—An amorphous metallic material. *Nanotechnology* **2016**, *27*, 035202. [CrossRef] [PubMed]

46. Shukla, N.K.; Mayet, A.M.; Vats, A.; Aggarwal, M.; Raja, R.K.; Verma, R.; Muqeet, M.A. High speed integrated RF–VLC data communication system: Performance constraints and capacity considerations. *Phys. Commun.* **2022**, *50*, 101492. [CrossRef]

47. Mayet, A.; Smith, C.E.; Hussain, M.M. Energy reversible switching from amorphous metal based nanoelectromechanical switch. In Proceedings of the 13th IEEE International Conference on Nanotechnology (IEEE-NANO 2013), Beijing, China, 5–8 August 2013; pp. 366–369.

48. Khaibullina, K. Technology to remove asphaltene, resin and paraffin deposits in wells using organic solvents. In Proceedings of the SPE Annual Technical Conference and Exhibition 2016, Dubai, United Arab Emirates, 26–28 September 2016.

49. Tikhomirova, E.A.; Sagirova, L.R.; Khaibullina, K.S. A review on methods of oil saturation modelling using IRAP RMS. *IOP Conf. Ser. Earth Environ. Sci.* **2019**, *378*, 012075. [CrossRef]

50. Khaibullina, K.S.; Korobov, G.Y.; Lekomtsev, A.V. Development of an asphalt-resin-paraffin deposits inhibitor and substantiation of the technological parameters of its injection into the bottom-hole formation zone. *Period. Tche Quim.* **2020**, *17*, 769–781. [CrossRef]

51. Khaibullina, K.S.; Sagirova, L.R.; Sandyga, M.S. Substantiation and selection of an inhibitor for preventing the formation of asphalt-resin-paraffin deposits. *Period. Tche Quim.* **2020**, *17*, 541–551. [CrossRef]

52. Mayet, A.M.; Alizadeh, S.M.; Kakarash, Z.A.; Al-Qahtani, A.A.; Alanazi, A.K.; Alhashimi, H.H.; Eftekhari-Zadeh, E.; Nazemi, E. Introducing a Precise System for Determining Volume Percentages Independent of Scale Thickness and Type of Flow Regime. *Mathematics* **2022**, *10*, 1770. [CrossRef]

53. Mayet, A.M.; Alizadeh, S.M.; Nurgalieva, K.S.; Hanus, R.; Nazemi, E.; Narozhnyy, I.M. Extraction of Time-Domain Characteristics and Selection of Effective Features Using Correlation Analysis to Increase the Accuracy of Petroleum Fluid Monitoring Systems. *Energies* **2022**, *15*, 1986. [CrossRef]

54. Taylor, J.G. *Neural Networks and Their Applications*; John Wiley & Sons Ltd.: Brighton, UK, 1996.

55. Gallant, A.R.; White, H. On learning the derivatives of an unknown mapping with multilayer feedforward networks. *Neural Netw.* **1992**, *5*, e129–e138. [CrossRef]

56. Roshani, M.; Sattari, M.A.; Ali, P.J.M.; Roshani, G.H.; Nazemi, B.; Corniani, E.; Nazemi, E. Application of GMDH neural network technique to improve measuring precision of a simplified photon attenuation based two-phase flowmeter. *Flow Meas. Instrum.* **2020**, *75*, 101804. [CrossRef]

57. Hosseini, S.; Roshani, G.H.; Setayeshi, S. Precise gamma based two-phase flow meter using frequency feature extraction and only one detector. *Flow Meas. Instrum.* **2020**, *72*, 101693. [CrossRef]

58. Roshani, M.; Ali, P.J.; Roshani, G.H.; Nazemi, B.; Corniani, E.; Phan, N.H.; Tran, H.N.; Nazemi, E. X-ray tube with artificial neural network model as a promising alternative for radioisotope source in radiation based two phase flowmeters. *Appl. Radiat. Isot.* **2020**, *164*, 109255. [CrossRef] [PubMed]

59. Peyvandi, R.G.; Rad, S.I. Application of artificial neural networks for the prediction of volume fraction using spectra of gamma rays backscattered by three-phase flows. *Eur. Phys. J. Plus* **2017**, *132*, 511. [CrossRef]

60. Roshani Gholam, H.; Ehsan, N.; Farzin, S.; Imani Mohammad, A.; Salar, M. Designing a simple radiometric system to predict void fraction percentage independent of flow pattern using radial basis function. *Metrol. Meas. Syst.* **2018**, *25*, 347–358.

61. Roshani, G.H.; Nazemi, E.; Feghhi, S.A.H.; Setayeshi, S. Flow regime identification and void fraction prediction in two-phase flows based on gamma ray attenuation. *Measurement* **2015**, *62*, 25–32. [CrossRef]